Am J Physiol Cell Physiol 285: C433–C445, 2003.
First published April 23, 2003; 10.1152/ajpcell.00509.2002.

Characterization of vectorial chloride transport pathways in the human pancreatic duct adenocarcinoma cell line HPAF

Peying Fong,[1] Barry E. Argent,[2] William B. Guggino,[1] and Michael A. Gray[2]

[1]*The Department of Physiology and Cystic Fibrosis Research Development Program, The Johns Hopkins University School of Medicine, Baltimore, Maryland 21205; and* [2]*School of Cell and Molecular Biosciences, Newcastle University Medical School, Newcastle-Upon-Tyne, United Kingdom NE2 4HH*

Submitted 5 November 2002; accepted in final form 18 April 2003

Fong, Peying, Barry E. Argent, William B. Guggino, and Michael A. Gray. Characterization of vectorial chloride transport pathways in the human pancreatic duct adenocarcinoma cell line HPAF. *Am J Physiol Cell Physiol* 285: C433–C445, 2003. First published April 23, 2003; 10.1152/ajpcell.00509.2002.—Pancreatic duct cells express a Ca^{2+}-activated Cl^- conductance (CaCC), upregulation of which may be beneficial to patients with cystic fibrosis. Here, we report that HPAF, a human pancreatic ductal adenocarcinoma cell line that expresses CaCC, develops into a high-resistance, anion-secreting epithelium. Mucosal ATP (50 μM) caused a fourfold increase in short-circuit current (I_{sc}), a hyperpolarization of transepithelial potential difference (from -4.9 ± 0.73 to -8.5 ± 0.84 mV), and a fall in resistance to less than one-half of resting values. The effects of ATP were inhibited by mucosal niflumic acid (100 μM), implicating an apical CaCC in the response. RT-PCR indicated expression of hClC-2, hClC-3, and hClC-5, but surprisingly not hCLCA-1 or hCLCA-2. K^+ channel activity was necessary to maintain the ATP-stimulated I_{sc}. Using a pharmacological approach, we found evidence for two types of K^+ channels in the mucosal and serosal membranes of HPAF cells, one activated by chlorzoxazone (500 μM) and sensitive to clotrimazole (30 μM), as well as one blocked by clofilium (100 μM) but not chromanol 293B (5 μM). RT-PCR indicated expression of the Ca^{2+}-activated K^+ channel KCNN4, as well as the acid-sensitive, four transmembrane domain, two pore K^+ channel, KCNK5 (hTASK-2). Western blot analysis verified the expression of CLC channels, as well as KCNK5. We conclude that HPAF will be a useful model system for studying channels pertinent to anion secretion in human pancreatic duct cells.

Ussing chamber; short-circuit current; RT-PCR; immunoblot

THE INHERITED DISEASE CYSTIC FIBROSIS (CF) takes its name from the pathological changes that occur in the pancreas (22). These changes include the appearance of precipitates in the pancreatic ductal tree, the formation of ductal cysts, and a generalized fibrosis that is probably caused by slow autodigestion of the gland. The factor that initiates these changes is a reduction in fluid and electrolyte secretion by the pancreatic ductal epithelium caused by mutations in the cystic fibrosis transmembrane conductance regulator (CFTR), a cAMP-activated Cl^- channel (41).

Activation of alternate Cl^- conductances has been proposed as a means by which CF-related organ disease may be either reduced or prevented. One functionally defined class of calcium-activated Cl^- conductances, here referred to collectively as CaCC, has been identified in a diverse range of epithelial cells (24, 34, 49) and, therefore, has emerged as a potential therapeutic target. Previous whole cell patch-clamp studies have demonstrated that a CaCC is expressed in mouse (25, 52) and human (51) pancreatic duct cells, as well as in HPAF cells, a human pancreatic ductal adenocarcinoma cell line (30, 51). Agonists that elevate intracellular calcium ($[Ca^{2+}]_i$) also increase iodide efflux from HPAF cells (1, 2, 31). Moreover, in two other pancreatic duct cell lines, PANC-1 and CFPAC-1, CaCC can drive appreciable HCO_3^- secretion (54). Therefore, a paradox exists as to why the pancreas is destroyed in CF, despite the fact that CaCC is expressed in duct cells and the evidence that this conductance can support anion secretion. Studying the characteristics and regulation of CaCC may indicate how the conductance could be activated so as to increase electrolyte and fluid secretion by the CF pancreas.

Previously, the regulation of CaCC in HPAF cells has been studied using nonpolarized monolayers (2, 31). In the present study, we have grown HPAF cells on permeable filters and used transepithelial electrical measurements in Ussing chambers, pharmacological probes, RT-PCR, and immunoblot analysis to address the following questions. First, do HPAF cells form an electrically tight, polarized epithelial sheet? Second, do HPAF cells exhibit vectorial anion transport under basal conditions and in response to agents that increase $[Ca^{2+}]_i$? Third, which Cl^- and K^+ channels are expressed in the mucosal and serosal membranes of HPAF cells?

MATERIALS AND METHODS

Transepithelial Transport Measurements

Cell culture. Briefly, HPAF cells (ATCC) between *passages 46* and *66* were plated, at a density of $2.5–5 \times 10^5$ cells/cm^2,

Address for reprint requests and other correspondence: P. Fong, Dept. of Physiology, The Johns Hopkins Univ. School of Medicine, Rm. 202C Physiology, 725 North Wolfe St., Baltimore, MD 21205 (E-mail: pfong@jhmi.edu).

The costs of publication of this article were defrayed in part by the payment of page charges. The article must therefore be hereby marked "*advertisement*" in accordance with 18 U.S.C. Section 1734 solely to indicate this fact.

on uncoated permeable polycarbonate membrane supports (Snapwell; Costar, Cambridge, MA). The cells were grown in a medium consisting of 90% Dulbecco's modified Eagle's medium and 10% fetal calf serum (GIBCO LTI) in a humidified, 37°C, 5% CO_2-95% air incubator. The growth medium was changed the day after plating and biweekly thereafter. Cells were maintained as stocks on uncoated, tissue-culture treated flasks. Experiments were performed on cells between *days 7* and *21* in culture.

Ussing chamber measurements. Monolayers were mounted on modified Ussing chambers [model CHM-5; World Precision Instruments (WPI), Sarasota, FL]. Both compartments were filled with phosphate-buffered saline (PBS) containing, (in mM) 140.0 NaCl, 2.0 $CaCl_2$, 1.2 $MgSO_4$, 0.375 KH_2PO_4, 2.125 K_2HPO_4, and 5.0 glucose, pH 7.4. The initial values for the transepithelial potential difference, resistance, and short-circuit current (V_t, R_t, and I_{sc}, respectively) were recorded before the chambers were bubbled with air. All measurements were carried out at 37°C. The V_t was monitored using 1 M KCl/agar, Ag/$AgCl_2$ cartridge electrodes (WPI), connected to an epithelial voltage clamp (model EC-825; Warner Instruments, Hamden, CT). Preselected constant current pulses were applied through similar 1 M KCl/agar, Ag/$AgCl_2$ cartridge electrodes. In most cases, measurements were performed under open-circuit conditions. The R_t was calculated in accordance with Ohm's law by dividing the magnitude of the voltage deflection, ΔV_t, by that of the applied current pulse, $I_{applied}$. That is,

$$R_t = \Delta V_t / I_{applied}$$

The equivalent short-circuit current, $I_{sc,eq}$, subsequently was calculated from the relationship

$$I_{sc,eq} = V_t / R_t$$

In some experiments, the short-circuited mode was employed, allowing a direct reading of the I_{sc}. Pulses of a known voltage were applied, resulting in current deflections that, by a similar calculation, yielded R_t. Taken together, the $I_{sc,eq}$ and I_{sc} measured under short-circuited conditions did not differ appreciably. Therefore, the data sets were pooled. For simplicity, the notation I_{sc} is used to indicate either $I_{sc,eq}$ or I_{sc} throughout the remainder of this report.

Several experiments tested the effects of boosting the Cl^- gradient across the apical membrane. In those experiments, the mucosal chamber was flushed carefully with a low Cl^- modification of the standard PBS; this solution substituted 140 mM Na-gluconate for NaCl. All other ionic replacements were made on an equimolar basis and have been specified appropriately when presented in RESULTS. The junction potential and fluid compartment resistance changes generated by Cl^- replacement were noted and corrected for in subsequent calculations of I_{sc}.

To stimulate transport, disodium ATP was added to a final concentration of 50 μM from a 50 mM stock prepared in PBS. Ionomycin, (1 μM; CalBiochem, La Jolla, CA) was added from a 1,000× dimethyl sulfoxide (DMSO) stock. In some instances, the effects of cAMP elevation were tested by adding isoproterenol (to a 10 μM final concentration from a 10 mM aqueous stock) or forskolin (to 10 μM final concentration from a 10 mM ethanolic stock) to the serosal chamber. The final concentration of 1 mM $BaCl_2$ was achieved by 1:1,000 dilution of a 1 M aqueous stock. Clofilium tosylate, clotrimazole, and niflumic acid were diluted to final concentrations (100, 30, and 100 μM, respectively) from 100 mM DMSO stocks. Chlorzoxazone was added to a final concentration of 500 μM from a 1,000× DMSO stock, and chromanol 293B was added from a 10 mM DMSO stock to a final concentration of 5 μM. Iberiotoxin and charybdotoxin were diluted to 5 nM (1:10,000) from 50 μM aqueous stocks. Experiments testing the above compounds were paired with the appropriate water, ethanol, or DMSO vehicle control experiments. Iberiotoxin and charybdotoxin were from Alomone Labs (Jerusalem, Israel). Chromanol 293B was a gift from Aventis Pharmaceuticals (Frankfurt, Germany). All other pharmacological agents were obtained from Sigma (St. Louis, MO).

Total RNA Preparation and RT-PCR

HPAF cells grown to confluence on uncoated flasks were washed twice with Ca^{2+}/Mg^{2+}-free PBS (GIBCO LTI) and removed by trypsinization. After addition of normal serum-containing growth medium to stop the digest, a cell pellet was obtained by centrifugation of the suspension at 800 rpm for 5 min and complete removal of the supernatant. The cell pellet was kept on ice until homogenization (QiaShredder; Qiagen, Valencia, CA) and total RNA isolation (QiaEasy; Qiagen) could proceed. After treatment with DNase I (Ambion, Austin, TX), RNA (0.4 μg) was random decamer-primed and reverse-transcribed using the SuperScript kit (Ambion), and PCR reactions were carried out with SuperTaq (Ambion) according to the manufacturer's instructions. In several experiments, RT-PCR was performed on an equivalent amount of total RNA from 16HBE14o- cells for the purpose of comparison.

All reverse transcriptions were executed in parallel with (−)RT controls. These latter reactions were used to control further for the possibility of genomic DNA contamination in the subsequent PCR reactions. Primer sequences specific for hClCA-1, hClCA-2, KCNQ1, and KCNN4, as well as optimal cycling conditions, were provided by, respectively, Drs. Catherine Fuller (University of Alabama, Birmingham, AL) and Elizabeth Cowley (Dalhousie University, Halifax, Nova Scotia, Canada). Primer sequences for ClC-3 and KCNK5 (hTASK2) were obtained from the literature (27, 29). Primer pairs directed toward both amino and carboxyl termini of hCFTR were a gift from Dr. Jie Cheng (Johns Hopkins University School of Medicine, Baltimore, MD). To control for the quality of the reverse transcriptions, reactions including primers for hClC-2, a ubiquitously expressed Cl^- channel, were also performed. All primer sequences and cycling parameters are summarized in Table 1. Primers were custom-synthesized (DNA Analysis Facility, Johns Hopkins University, and Invitrogen Life Technologies, Carlsbad, CA). PCR runs always included a minus (−) template control reaction, substituting an equal volume of tissue culture grade, deionized water (GIBCO LTI) for reverse transcription reaction.

Preparation of Total Cell Lysate

T25 flasks containing monolayers of HPAF cells were chilled by placement on ice. The growth medium was removed by aspiration, and the cells were then washed twice with ice-cold, divalent-free PBS. Lysis buffer (100 μl) consisting of 50 mM Tris·HCl, 150 mM NaCl, 1% NP-40, 0.5% Na-deoxycholate, pH 7.5, plus Complete protease inhibitor cocktail (1 tablet per 50 ml lysis buffer; Boehringer) was added to each T25 flask. The flasks were gently tilted to cover the growth surface completely with the lysis buffer and then placed on ice for 10 min. After vigorous scraping, the lysate was collected and transferred to prechilled tubes and then spun at 10,000 *g* for 1 min at 4°C to pellet-insoluble material. The supernatant was collected and transferred to tubes for storage at −20°C before quantification of protein concentra-

Table 1. *Primers and conditions for RT-PCR*

Primer Specific for	Primer Sequence (5′ to 3′)	Cycling Conditions (Denaturation, Annealing, Extension)	Predicted Fragment Size, bp
hCFTR, COOH terminus	F: ACGCGTCGACGAGAATGATGATGAAGTACAG R: ATAAGAATGCGGCCGCGCTATTGAAGTAT CTCACAT	(Melt, 94°C, 2 min) 94°C/30 s; 55°C/30 s; 72°C/45 s; 30 cycles (extend, 72°C, 5 min)	175
hCFTR, NH_2 terminus	F: ACGCGTCGACGATGCAGAGGTCGCCTCTGG R: ATAAGAATGCGGCCGCTCTCCAGAAAAAACA TCGCC	Same as above	221
hClC-2	F: CTGCCCTACCTGCCTGAGC R: CTCTTCAGGGCTCATCTCG	Same as above	626
hClC-3*	F: CACAGCACACCCCATCTC R: CTCCCCAAACAACTCCTC	Same as above	443/ClC-3a 519/ClC-3b
hClC-5	F: CCCGGGAGTCCCAAAGAC R: GAAGAGAATGGAATCAGG	Same as above	361
hClCA-1†	F: AGGCTGACTATGTGAGACCAA R: GCCTCCCTGACACTTCTTTA	95°C/30 s; 51°C†/30 s; 72°C/45 s; 35 cycles	345
hClCA-2†	F: CCAAAGGAGCATTGCAGGTC R: ATCTCCATGTGCCCCATACC	95°C/30 s; 45°C†/30 s; 72°C/45 s; 35 cycles	360
KCNQ1‡	F: TTCTGGATGGAGATCGTG R: GCCTTCCGGATGTAGATC	95°C/30 s; 63°C/1 min; 72°C/1 min; 35 cycles	738
KCNN4‡	F: CGGCGTCCTGCTCAACG R: CACCAGCAGGGCTGTGCAG	95°C/1 min; 62°C/30 s; 72°C/90 s; 30 cycles	337
KCNK5§	F: CTGCTCACCTCGGCCATCATCTTC R: GTAGAGGCCCTCGATGTAGTTCCA	(Melt, 94°C, 2 min) 94°C/30 s; 55°C/30 s; 72°C/45 s; 30 cycles (extend, 72°C, 5 min)	566

Highlighted areas of cystic fibrosis transmembrane regulator (CFTR) primers are tag regions (not CFTR specific). *Primer sequences from Ref. 38. †Primers and annealing temperatures suggested by Dr. C. Fuller (unpublished observations). ‡Primer sequences and cycling parameters from Ref. 17. §Primers from Ref. 40.

tion by bicinchoninic acid assay (Pierce, Rockford, IL), electrophoresis, and immunoblotting.

Electrophoresis and Immunoblotting

Proteins contained in HPAF total cell lysate (100 μg) were separated by SDS/PAGE on Tris·HCl gels of the appropriate polyacrylamide concentrations (7.5 or 12%; Ready-Gels; Bio-Rad, Hercules, CA) and then transferred onto polyvinylidene difluoride membranes (Bio-Rad). ClC-2 and ClC-3 (3A6) antibodies were generously provided by Prof. Thomas J. Jentsch (Zentrum für Molekulare Neurobiologie, Hamburg, Germany). Prof. Olivier Devuyst (Université Catholique de Louvain, Brussels, Belgium) kindly made available the ClC-5 antibody, as well as the peptide antigen for use in negative control experiments. A peptide specific to the carboxyl terminus of ClC-2 was obtained from Alomone Labs (Jerusalem, Israel), as were the antibody against KCNK5 (hTASK-2) and its control antigen. ClC-2 and ClC-3 primary antibodies were used at a dilution of 1:500, whereas the ClC-5 antibody was diluted at 1:1,000. Anti-KCNK5 was used as recommended by the manufacturer (1:200 dilution of 0.3 mg/ml). In all cases, we used a horseradish peroxidase (HRP)-labeled donkey anti-rabbit secondary antibody at a dilution of 1:3,000 (Amersham). Detection was by enhanced chemiluminescence (ECL) after introduction of HRP substrate (Amersham ECL Western blot detection kit or Perkin Elmer Lightning detection kit). All immunoblot data are presented as unenhanced scans of the primary films.

Statistical Analysis

Data are presented as means ± SE. Unless otherwise specified, the effects of pharmacological agents were studied in paired monolayers, and statistical significance was determined by Student's paired *t*-test. We assigned significance at $P < 0.05$.

RESULTS

Resting Electrical Properties of HPAF Cells

Under open-circuited conditions, HPAF cells displayed a spontaneous negative resting V_t of −4.9 ± 0.73 mV ($n = 23$), indicating either basal anion secretion or cation absorption. The resting R_t of HPAF cells was 1,471 ± 180 Ω·cm^2 ($n = 23$), which is high compared with values reported for CFPAC-1 (290 ± 12 Ω·cm^2; Ref. 7) and CAPAN-1 cells (119 ± 9.7 Ω·cm^2; Ref. 9). The resting I_{sc} was 3.93 ± 0.33 μA·cm^{-2} ($n = 29$), which, although higher than the I_{sc} measured in CAPAN cells (1.32 ± 0.37 μA/cm^2; Ref. 9), agrees well with that observed previously in CFPAC-1 cells (4.0 ± 1.2 μA/cm^2; Ref. 7). Consistent with the findings of Novak and Hansen (37), who reported no functional epithelial Na^+ channel (ENaC) in rat pancreatic ducts, mucosal amiloride (10 μM; $n = 5$) had no effect on the electrical parameters. Moreover, confluent monolayers

grown on plastic showed no evidence of dome formation. Thus HPAF cells form a tight, anion-secreting epithelium.

Effect of cAMP-Elevating Agents

To determine the contribution of cAMP-mediated conductances to the net secretory response of HPAF monolayers, either isoproterenol (10^{-5} M) or forskolin (10^{-5} M) was applied to the serosal solution. In symmetrical, Cl^- replete solutions, these agents elicited a slight increase in I_{sc} that rarely exceeded 0.5 μA (n = 6). On imposition of a large, mucosally directed Cl^- gradient by replacement of 140 mM mucosal NaCl with Na-gluconate, a discernable but still negligible increase (of ~1 μA; n = 3) in secretory current resulted when either agonist was added. The inclusion of 25 mM HCO_3^- in the mucosal and serosal solutions had no effect on either resting I_{sc} or on the cAMP response (n = 4 pairs, P = 0.1 by paired t-test). Taken together, these data indicate that at best, cAMP-mediated Cl^- conductances, such as CFTR, play a minor role in the total secretory response of HPAF cells.

Effect of Calcium-Elevating Agents

To address whether CaCC can mediate a Cl^- secretory response in polarized HPAF cells, we tested the effects of calcium-elevating agents. Figure 1 summarizes the response to mucosal ATP. The application of 50 μM ATP to the mucosal compartment resulted in a complex series of electrical changes. Initially, ATP often produced a rapid, transient depolarization that then rebounded promptly, hyperpolarizing V_t to −8.5 ± 0.84 mV (n = 23 monolayers) (Fig. 1*A*). During the hyperpolarization, the R_t fell to less than one-half that of resting values, 628 ± 67.2 Ω·cm^2 (n = 23) (Fig. 1*B*). In the recovery phase, the V_t slowly depolarized before returning to near-resting values; during this period, R_t steadily increased to that of the unstimulated monolayer. The typical change in I_{sc} was biphasic (example shown in Fig. 1*C*). By 50 s post-ATP addition, the response peaked at 15.4 ± 1.23 μA/cm^2 (n = 29) (Fig. 1*D*) and then decayed steadily so that the I_{sc} was one-half maximal by ~5 min, reaching essentially resting levels after 15 min. Like the response to cAMP agonists, baseline and ATP-stimulated I_{sc} was insensitive to the presence or absence of HCO_3^- (n = 5 pairs, P = 0.3 by paired t-test).

Role of Cl^- Channels in the Generation of I_{sc}

Consistent with the reported pharmacology of CaCC in HPAF cells (51), the mucosal addition of 100 μM niflumic acid shortly (150 s) after achievement of peak values produced a clear drop in the I_{sc} (Fig. 2*A*). Niflumic acid also produced a distinct drop in the I_{sc} when added after the peak current had almost completely decayed (10 min; see also Fig. 2*B*). We also verified that the ATP response was due to Cl^- secretion by performing Cl^- substitution experiments. Under open-circuited conditions, the imposition of a serosal to mucosal Cl^- gradient by replacement of mucosal Cl^- with gluconate did not significantly change the resting I_{sc} (P = 0.3). Monolayers in symmetrical Cl^- solutions increased I_{sc} by 8.82 ± 0.99 μA/cm^2 in response to ATP. In the presence of a Cl^- gradient, the ΔI_{sc} was significantly greater, 17.84 ± 1.75 μA/cm^2 (P < 0.03 by paired t-test; n = 5 tissue pairs). Taken together with previously published findings that show both ionomycin and ATP stimulate iodide efflux from HPAF cells (31, 51), our data indicate that the ATP-induced increase in I_{sc} involves activation of Cl^- channels.

Interestingly, HPAF monolayers bathed in symmetrical Cl^- solutions did not respond to more than one exposure to ATP. To understand better whether this resulted from desensitization of the CaCC or an inability of the cells to accumulate Cl^- sufficiently, we replaced mucosal NaCl with Na-gluconate and, after

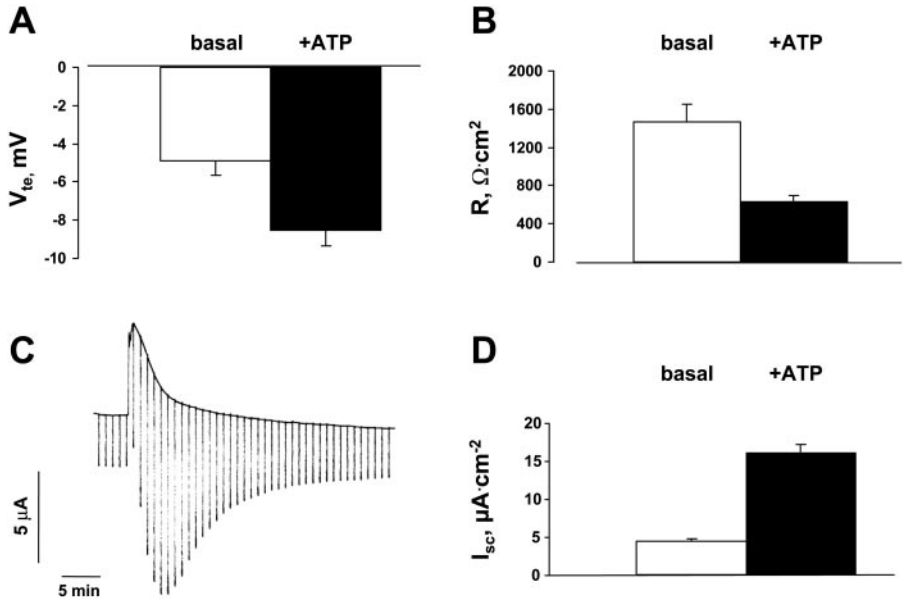

Fig. 1. Resting and ATP-stimulated electrical properties of HPAF cells. In *A*, *B* and *D*, the open bars indicate basal levels, whereas the solid bars indicate peak ATP stimulated levels. *A*: summary of transepithelial potential difference (V_t) values. *B*: transepithelial resistance (R_t). For both, n = 23. *C*: original trace showing a typical short-circuit current (I_{sc}) response to 50 μM mucosal ATP in a directly short-circuited monolayer. Current deflections reflect response to −10-mV voltage pulses. *D*: summary of basal and ATP stimulated I_{sc}; data are means ± SE and n = 29.

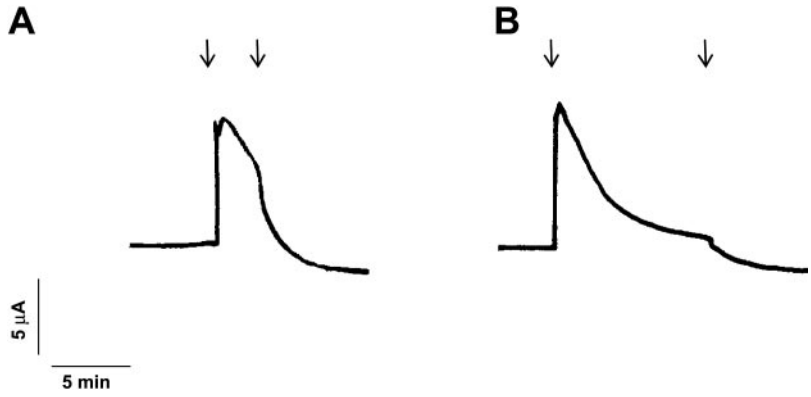

Fig. 2. ATP-stimulated I_{sc} is blocked by niflumic acid (NA). In each trace, the time at which 50 μM ATP was added to the mucosal chamber is indicated by the first arrow and the addition of NA is indicated by the second arrow. Mucosal NA (100 μM) inhibited ATP-stimulated I_{sc} at ~150–200 s (*A, left*) and ~10 min (*B, right*) after addition of ATP. Resting I_{sc} values were 5 and 5.6 μA/cm^2, for *A* and *B*, respectively.

stabilization, again applied 50 μM ATP. Imposing a mucosal Cl^- gradient permitted resolution of an abbreviated, but clearly discernable, second response to ATP (n = 4 experiments). These data suggest that in Cl^- replete solutions, intracellular Cl^- falls to equilibrium after ATP stimulation. However, they do not rule out, a priori, a role for receptor desensitization in either this process or in the decay of ATP-stimulated I_{sc}.

Ionomycin (1 μM) produced qualitatively similar changes to ATP (n = 5 experiments), although the decay of I_{sc} appeared more rapid. We did not investigate this point further.

Role of K^+ Channels in the Generation of I_{sc}

The epithelial K^+ conductance, G_K, limits Cl^- secretion. A vast array of K^+ channel families have been identified and categorized based on *1*) the molecular family to which they belong, *2*) their electrophysiological signature, and *3*) their pharmacological modulation. Multiple species have been shown to be important in the secretory response of a variety of epithelial cell lines, including Calu-3, HCA-7/Colony 1, and T-84 (17, 19, 27, 34), as well as native tissues. As a first step toward identifying the major K^+ channel types underlying the Cl^- secretory response in HPAF cells, we have tested the I_{sc} inhibitory effects of several agents previously demonstrated to block distinct K^+ channel species.

Initially, the block of I_{sc} by a relatively nonspecific agent, $BaCl_2$, was assessed. In these experiments, the composition of the PBS was modified, replacing $MgSO_4$ with $MgCl_2$ to prevent the precipitation of barium salts. The serosal addition of $BaCl_2$ (1 mM) to unstimulated monolayers did not affect basal I_{sc} (3.27 ± 0.315 μA/cm^2, control, vs. 3.16 ± 0.353 μA/cm^2, $BaCl_2$; P > 0.3, n = 5). Further addition of mucosal $BaCl_2$ did not alter the response. The ATP-stimulated I_{sc} was not different between control monolayers and those bilaterally exposed to $BaCl_2$ (13.25 ± 3.188 μA/cm^2, control, vs. 9.71 ± 1.37 μA/cm^2, $BaCl_2$; means ± SE; P > 0.19, n = 8).

Clotrimazole is an inhibitor of Ca^{2+}-activated K^+ channels (19). Although either serosal or mucosal clotrimazole (30 μM) alone decreased resting I_{sc} (~20–30%), bilateral addition produced optimal inhibition. Figure 3, *A* and *B*, shows that adding 30 μM clotrimazole to both serosal and mucosal chambers significantly reduced the baseline I_{sc} from 3.75 ± 0.82 to 2.25 ± 0.63 μA/cm^2 (40% block; P < 0.05; n = 6 monolayer pairs). The peak ATP-activated secretory current decreased from 11.87 ± 1.61 to 6.75 ± 1.44 μA/cm^2 (P < 0.05; n = 6 pairs of control and clotrimazole pretreated monolayers). After ATP stimulation, the mucosal addition of clotrimazole inhibited I_{sc} in a manner indistinguishable from that produced by niflumic acid (compare Fig. 3*C* with Fig. 2*A* and Fig. 3*D* with Fig. 2*B*).

Interestingly, the mucosal addition of chlorzoxazone (500 μM), an activator of small and intermediate conductance Ca^{2+}-activated K^+ channels (46), significantly increased the resting I_{sc} about threefold from 4.21 ± 0.25 to 14.79 ± 1.11 μA/cm^2 within 10 min of application (Fig. 4*A*; n = 13 monolayers). In contrast, serosal application of chlorzoxazone (500 μM) had no effect (Fig. 4*B*). Neither mucosal nor serosal addition of DMSO alone (the solvent for chlorzoxazone) had any effect on I_{sc} (Fig. 4, *A* and *B*). In monolayers stimulated with mucosal chlorzoxazone, subsequent addition of apical clotrimazole restored I_{sc} to within 10% of baseline levels (Fig. 4*C*), inhibiting the chlorzoxazone-stimulated current by 89.2 ± 5.98% (n = 6 monolayers; Fig. 4*D*).

After chlorzoxazone treatment, mucosal ATP produced a typical biphasic increase in I_{sc}, the peak magnitude of which did not differ significantly from that measured in paired DMSO-treated controls (7.6 ± 0.73 vs. 5.8 ± 0.67 μA/cm^2, chlorzoxazone vs. control; P > 0.1, n = 3 monolayer pairs). Moreover, compared with the controls, the absolute I_{sc} block by clotrimazole was greater in the chlorzoxazone-treated monolayers. When applied 15 min post-ATP peak and measured 10 min after application, clotrimazole decreased I_{sc} in chlorzoxazone-treated monolayers by 3.8 ± 0.44 vs. 1.6 ± 0.41 μA/cm^2 in DMSO controls (P < 0.05, n = 3 pairs).

We next sought to test the involvement of cAMP-dependent K^+ channels. Figure 5 shows that mucosal addition of clofilium (100 μM), an inhibitor of cAMP-gated K^+ channels in Calu-3 cells (17), significantly decreased baseline I_{sc} from 4.07 ± 0.470 to 2.53 ±

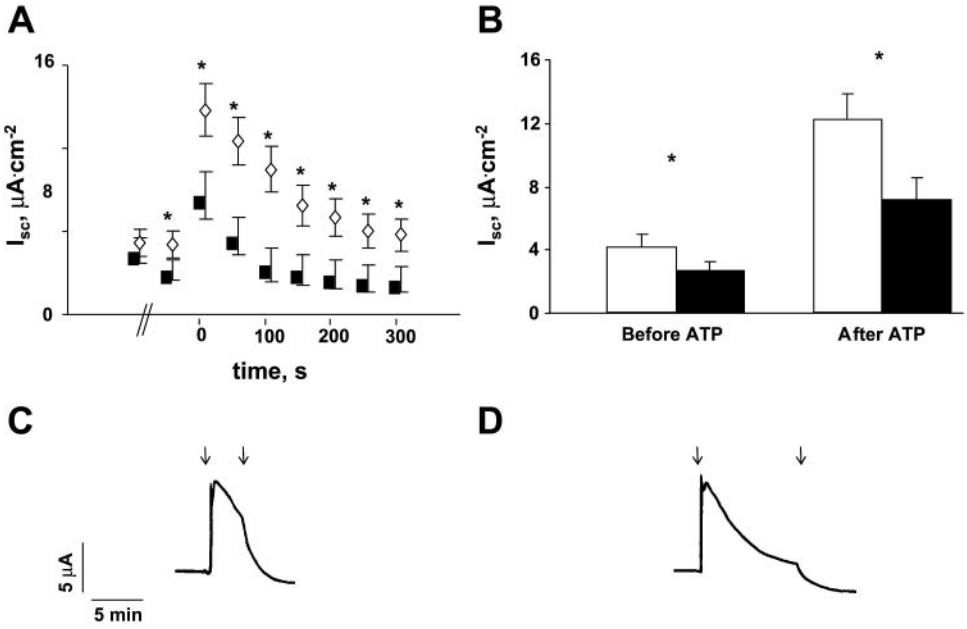

Fig. 3. Effects of bilateral clotrimazole (CLT). *A*: early time course of I_{sc} changes. Open symbols indicate DMSO control tissues, and closed symbols represent values from tissues pretreated with 30 μM CLT. The point before the hatch marks indicates resting I_{sc} levels and that immediately following indicates the basal values after either DMSO or CLT treatment. ATP (50 μM) was then added to the mucosal chamber. *Time 0* indicates the time at which the peak I_{sc} value was achieved. *Statistical significance ($P < 0.05$) between the two data sets, as determined by paired *t*-test ($n = 6$ monolayer pairs). *B*: summary comparison of the resting and ATP peak I_{sc} values for control (open bars) and CLT-treated (solid bars) monolayers. *C* and *D* show that ATP-stimulated I_{sc} is blocked by mucosal CLT (30 μM). In both, 50 μM ATP was added to the mucosal chamber at the time indicated by the first arrow; the addition of CLT is indicated by the second arrow. *C* shows the response to 30 μM mucosal CLT added ~150–200 s post-ATP, whereas *D* depicts the block when added 10 min after ATP stimulation. Note that for comparison with the niflumic acid data in Fig. 2, the response shown in *C* was obtained on the same day as that in Fig. 2*A*, whereas that in *D* was recorded on the same day as that in Fig. *2B*. Resting I_{sc} values were 4.7 and 5.4 μA·cm^{-2} for *C* and *D*, respectively.

0.116 μA/cm^2 ($P < 0.05$; $n = 3$ pairs), whereas paired DMSO controls showed no change (4.17 ± 0.033 μA before vs. 4.07 ± 0.067 μA after; $P > 0.1$; $n = 3$ pairs). Treatment with clofilium had no effect on the mean peak response to mucosal ATP addition ($P > 0.2$ for a comparison between 3 tissue pairs). Thirty minutes post-ATP stimulation, control monolayers recovered ~75% of their resting R_t and, as shown in Fig. 5, I_{sc} was indistinguishable from unblocked baseline levels. In contrast, those monolayers treated with clofilium scarcely recovered 30% of resting R_t and showed an accompanying diminishment of I_{sc}. The mucosal addition of clofilium after stimulation by ATP also decreased I_{sc} ($n = 3$ experiments, addition at ~150 s after ATP peak; $n = 6$, addition at 30 min post-ATP peak; data not shown). Neither resting, stimulated, nor post-stimulated I_{sc} were affected by the serosal application of clofilium.

To further characterize the K^+ conductance in HPAF cells, we studied the effects of chromanol 293B, a compound with greater specificity for cAMP-activated K^+ conductances. Surprisingly, 293B at 5 μM, a concentration that effectively blocks cAMP-activated KCNQ1/KCNE3 type K^+ channels (3), had no effect on basal I_{sc} when added to either side of the HPAF monolayer ($n = 4$).

Finally, neither mucosal nor serosal application of the maxi-K^+ channel inhibitors charybdotoxin and iberiotoxin (5 nM, respectively) affected basal, ATP stimulated, or chlorzoxazone-stimulated I_{sc} ($n = 5$ experiments). We therefore ruled out a contribution of this class of K^+ channels to the Cl^- secretory response.

RT-PCR Analysis of Channel Expression

As a first step toward the molecular identification of the channels underlying these functional observations, we undertook RT-PCR analysis. Primers specific for the following Cl^- channels were tested: human CFTR, ClC-3, ClC-5, CLCA-1, and CLCA-2. In addition, reactions designed for the detection of the ubiquitously expressed Cl^- channel, ClC-2, were utilized as positive controls. To elucidate the molecular identity of the clofilium-sensitive component of basal I_{sc}, we carried out reactions with primers specific for *1*) KCNQ1, a species that, along with any of several tissue-specific KCNE subunits, comprises a cAMP-mediated K^+ channel in many epithelial cells, including those of gastrointestinal and airway origin (17, 43), and *2*) KCNK5 (hTASK-2), an acid-sensitive, four-transmembrane domain, two-pore (4TMD-2P) K^+ channel found recently to participate in regulatory volume decrease (35). To identify the clotrimazole-sensitive basal and ATP-

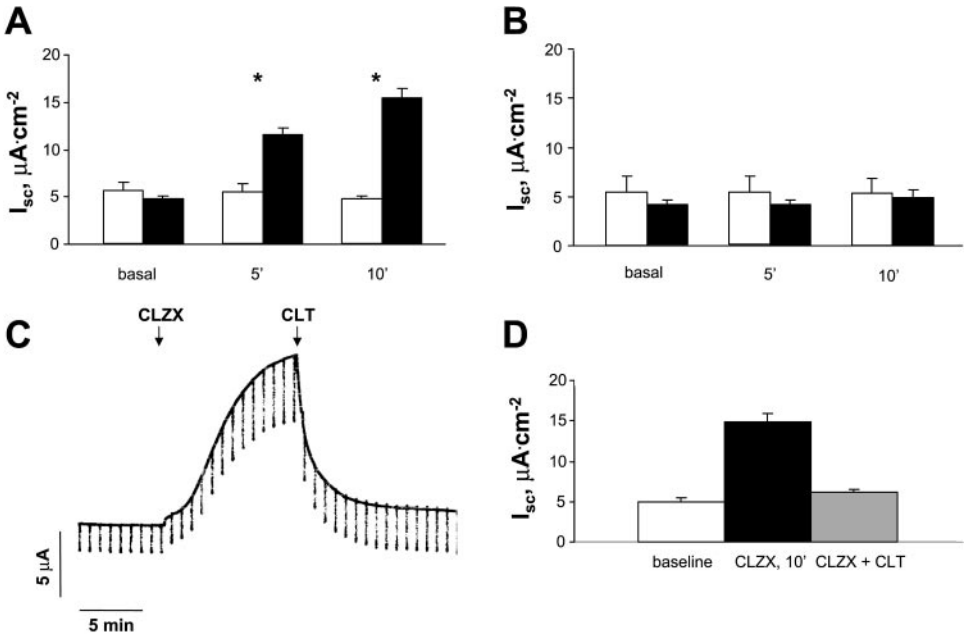

Fig. 4. *A*: effect of 500 μM mucosal chlorzoxazone (CLZX; solid bars) on I_{sc} at $t = 0$ min (basal; *left*), 5 min (*middle*) and 10 min (*right*). Open bars represent data from DMSO controls. Data are means ± SE. For CLZX-treated monolayers, $n = 13$, whereas $n = 11$ for DMSO-treated monolayers. *$P < 0.0005$, by 2-tailed t-test. *B*: lack of effect of the same concentration of CLZX when applied to the serosal chamber. DMSO and CLZX data bars represented by open and solid bars, respectively. Order of data bars remains as in *A*. Data are means ± SE, $n = 3$, for each set. By 2-tailed t-test, $P > 0.5$, and therefore data are not significantly different. *C*: original data trace showing effective block of CLZX-augmented I_{sc} by 30 μM mucosal clotrimazole (CLT). *D*: summary of results showing effective inhibition of CLZX-stimulated I_{sc} by mucosal CLT. Open bars represent mean baseline I_{sc}, solid bars indicate mean values 10 min post-CLZX, and gray bars show the level after CLT. Error bars are SE values; $n = 6$ monolayers.

stimulated current component, we also used primers specific for the Ca^{2+}-activated K^+ channel, KCNN4 (29).

RT-PCR using primer pairs specific for either amino or carboxyl termini of hCFTR yielded faint bands of the predicted sizes that were absent in negative control reactions, indicating the weak expression of mRNA encoding CFTR in HPAF cells (Fig. 6*A*; parallel reactions of total RNA from 16HBE14o$^-$ cells used as a positive control). Quite surprisingly, neither hCLCA-1 nor -2 primers produced any product over a range of cycling conditions (data not shown). On the other hand, reactions with ClC-2, ClC-3, and ClC-5 primer pairs indicated substantial expression (Fig. 6*B*). Reactions using the KCNQ1, KCNK5, and KCNN4 primers indicated the presence of mRNA encoding all three K^+ channel species, albeit to varying degrees. KCNQ1 appeared very weakly (see comparison with signal in 16HBE14o$^-$ cells, Fig. 6*C*). This finding agrees well with the functional data showing no effect of chromanol 293B on I_{sc}. Reactions using primers for both KCNK5 (hTASK2) and KCNN4 indicated that HPAF cells express both of these K^+ channels abundantly (see Fig. 6*C*).

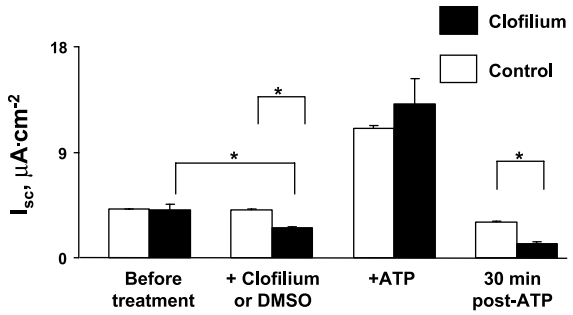

Fig. 5. Effect of mucosal clofilium. Data from DMSO vehicle control monolayers are shown for comparison. Bars represent means ± SE, $n = 3$ pairs of monolayers for each set. *Significance ($P < 0.05$) as determined by paired, 2-tailed t-test.

Immunoblot Analyses to Test for the Presence of Cl^- and K^+ Channel Proteins

Our RT-PCR findings suggest the possibility that three members of the CLC family of Cl^- channels may play roles in either or both the basal and stimulated Cl^- conductance of HPAF cells. They also identify KCNN4 as the molecular species underlying the clotrimazole-inhibited, CLZX-stimulated K^+ current that is necessary for sustaining ATP-activated secretion and KCNK5 as a novel, apically localized, background K^+ channel. Because protein expression cannot be assumed from positive RT-PCR results, we undertook Western blot analysis to test for the presence of these channel proteins in HPAF cells.

As shown in Fig. 7*A*, HPAF total cell lysate showed immunoreactivity to an affinity-purified antiserum

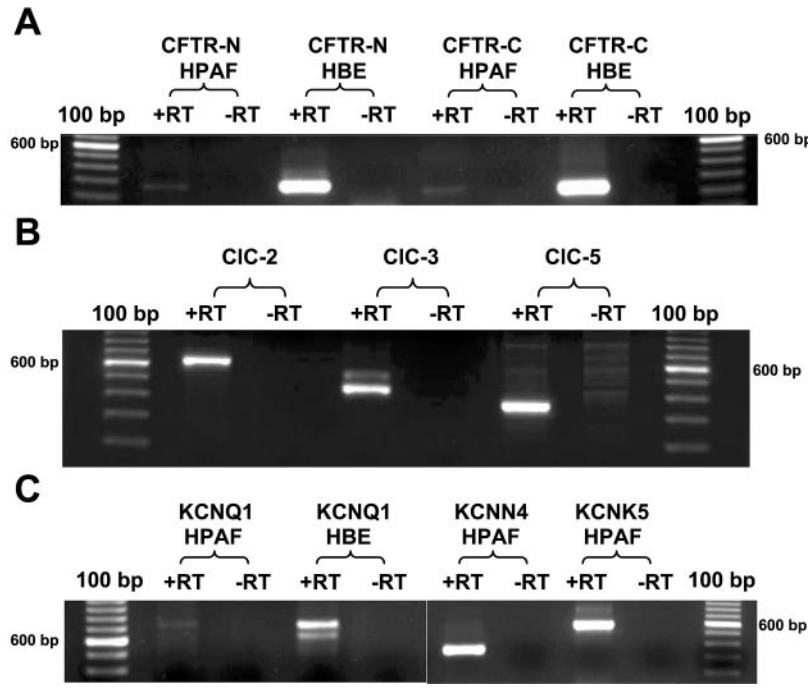

Fig. 6. RT-PCR of HPAF total RNA. 1.2% agarose/Tris-acetate-EDTA (TAE) gels of PCR products for (+) and (−) reverse transcriptase reactions were run, with 100 base pair ladders shown in the *left* lane. All reactions used 3 μl of RT product in the subsequent PCR reactions (50-μl reaction volumes). Nine microliters of reaction product were run in each lane. *A*: the expression of CFTR in HPAF cells with that in 16HBE14ō cells is compared. *B*: expression of ClC-2, -3, and -5; note the presence of the 2 alternatively spliced forms of ClC-3. *C*: the products of reactions using primers specific for KCNQ1, KCNN4, and KCNK5. *Left*: overexposure reveals low expression of KCNQ1 in HPAF cells vs. abundant expression in 16HBE14ō cells. All reactions used primer pairs and cycling conditions given in Table 1.

specific for the ubiquitously expressed CLC channel, ClC-2 (*lane 3*). This well-characterized antibody has previously been shown to react with testis and retinal lysates obtained from wild-type, but not ClC-2-knockout, mice (5). We used a total protein extract from mouse testis as a positive control (*lane 1*). Whereas the size of the predominant band in this preparation was slightly smaller than the expected molecular mass of ~100 kDa (arrow), the independent findings of several other groups indicate that ClC-2-specific bands migrate between ~80 and 100 kDa. These differences may arise from either tissue-specific splicing or variations in glycosylation. Moreover, species differences may contribute to the size difference by exerting an influence on either or both of the above variables. In addition to the ~100-kDa band in the HPAF lane, we also note the presence of a smaller band. Although the antigen against which this antibody was produced was unavailable, its sequence (HGLPREGTPSDSDDKCQ) significantly overlaps that of a commercially available ClC-2 COOH terminus peptide (RSRHGLPREGTPSDSDDKC; regions of overlap underlined). Thus peptide displacement experiments (*lanes 2* and *4*) allowed us to confirm that the bands in both the testis and HPAF lanes most likely represent ClC-2 protein, as well as to ascertain that the smaller band in the HPAF lane indeed reflects a (specific) degradation product rather than nonspecific binding (compare *lanes 3* and *4*). Figure 7*B* shows, using an antibody generated against ClC-3 (3A6; 48), the presence of that channel protein in HPAF cells (*right lane*); as a positive control, the signal from rat cerebellar lysate is shown for comparison (*left lane*). The slight discrepancy in molecular mass is consistent with previous findings made using this antibody on various mouse tissue lysates, including brain and pancreas (48).

Immunoblot analysis also confirmed the presence of ClC-5 in HPAF cells (Fig. 7*C*). Compared with the characteristically broad band that is detected in total kidney extract, that found in HPAF cells is more uniform and, on average, of slightly higher molecular mass. Such differences can be attributed to possible cell/tissue-specific glycosylation, anomalous electrophoretic mobility (20), and even potentially ubiquitination (44). Importantly, preincubation of the antibody with the peptide antigen completely abolished the signal.

Although we were unable to locate a source for antibody against KCNN4, we did obtain a commercial antibody against KCNK5 (Alomone Labs). As shown in Fig. 7*D*, strong immunoreactivity was obtained with a band detected at the predicted molecular mass of ~55 kDa (*left lane*). In addition, a lower molecular mass band running slightly above 30 kDa most likely represents a degradation product, because it, too, was abolished when the peptide-blocked antibody was used (see *right lane*).

DISCUSSION

Our data show that HPAF cells grown on permeable supports develop into epithelial monolayers that secrete Cl^-. We were unable to detect a stimulation of I_{sc} in HPAF monolayers by cyclic AMP and only detected weak expression of CFTR using RT-PCR. Chambers and Harris (8) previously screened for CFTR in several pancreatic adenocarcinoma lines using RT-PCR. Whereas most lines, including HPAF, showed no CFTR transcript, this species was detected in CAPAN-1 cells. Interestingly, levels of RNA encoding CFTR in CAPAN-1 cells varied as a function of confluence. These authors did not test whether increasing HPAF

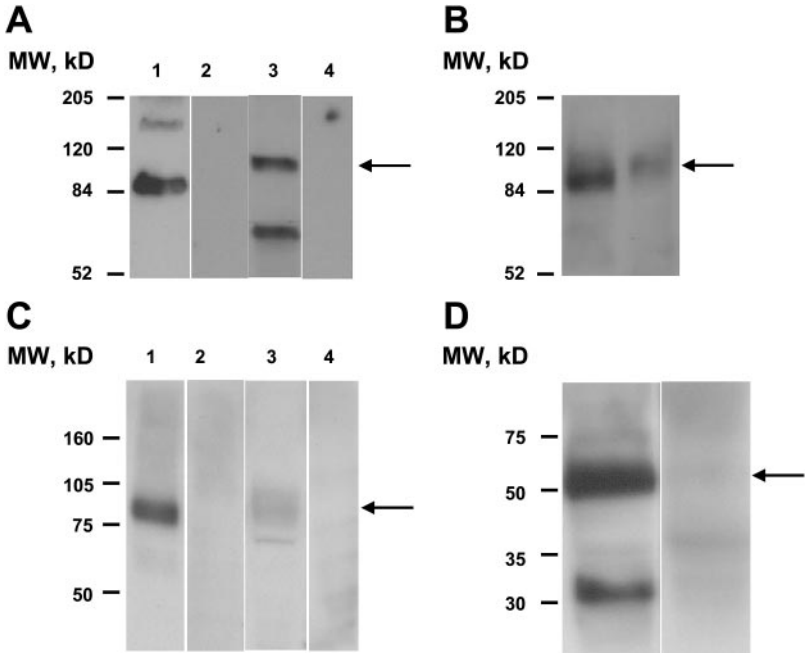

Fig. 7. Immunoblot analysis for ClC-2 (*A*), ClC-3 (*B*), ClC-5 (*C*), and KCNK5 (hTASK2) (*D*). *A*: total HPAF cell lysate (~100 μg each; *lanes 3* and *4*) was separated by SDS-PAGE, transferred to a polyvinylidene difluoride membrane, and probed with either an affinity-purified rabbit polyclonal antiserum directed against a COOH-terminal peptide specific to the ubiquitous CLC channel, ClC-2, or peptide-blocked antibody (*lane 4*). The antibody was used at 1:500 dilution. *Lanes 1* and *2* show, respectively, the test and peptide-blocked signals from the positive control, total lysate (100 μg/lane) obtained from mouse testis (5). The arrow indicates a product corresponding to the predicted molecular mass of ClC-2 (~100 kDa). *B* shows an immunoblot probed with a rabbit polyclonal antiserum (3A6) directed against an NH_2-terminal peptide specific to ClC-3 (48). The *right lane* shows the signal in 100 μg HPAF total cell lysate. Shown for comparison is the reactivity obtained using an equal amount of rat cerebellar lysate (*left lane*). *C*: Western blot using rabbit polyclonal antiserum to a COOH-terminal peptide of ClC-5. *Lanes 1* (positive control; 10 μg total rat kidney homogenate) and *3* (100 μg total HPAF cell lysate) were probed with 1:1,000 dilution of the primary antibody. *Lanes 2* and *4* contain 10 μg of total rat kidney homogenate and 100 μg HPAF cell lysate, respectively, and were probed with the peptide-blocked antibody. *D*: HPAF lysate (100 μg) probed with anti-KCNK5 (Alomone Labs) at a 1:200 dilution of a 0.3 mg/ml stock. The arrow indicates the band migrating at the predicted molecular mass of KCNK5, ~55 kDa. The *left lane* is the result of incubation with primary antibody; the *right lane* is the negative control using the antigen-blocked antibody. For further discussion, see text.

cell confluence also increased CFTR transcripts, which may explain the discrepancy between their study and our present findings. Although this will be interesting and important to test in future studies, we have not yet implemented quantitative, real-time PCR measurements to ascertain whether CFTR expression increases in a time-dependent fashion once confluency is achieved. The rather higher R_t observed in the HPAF cell line compared with other human ductal cell lines that retain epithelial function may, in part, be explained by weak expression of CFTR.

What distinguishes HPAF cells from previously characterized lines? In recent years, it has become evident that different classes of CF mutations correlate with the severity of disease (11). On one end of the spectrum are the class I–III mutations; these are associated with lung disease and pancreatic insufficiency. Trafficking mutants such as ΔF508 fall into class II. On the other end are the class IV (altered conductance) and V (reduced synthesis) mutations; these patients are pancreatic sufficient. CFPAC-1 cells originate from a ΔF508/ΔF508 CF patient and occupy an established place in studies directed at understanding the effects of trafficking mutants on ductal function (42). The CAPAN-1 line, in contrast, expresses substantial levels of CFTR and, hence, serves in most studies as the wild type control. Like CAPAN-1 cells, HPAF cells originate from a non-CF individual. However, we report here that HPAF cells have a much reduced expression of CFTR, thus making them a potential model for class V CF mutations. Individuals affected with class V mutations are often asymptomatic but are often identified when presenting with idiopathic pancreatitis or congenital bilateral absence of vas deferens (10, 12, 14, 15, 21). We therefore suggest that the HPAF line may prove useful in studies directed at understanding the pathophysiology of these conditions.

Interestingly, the presence of HCO_3^- affects neither cAMP nor Ca^{2+}-stimulated I_{sc} profoundly in HPAF cells. Greely et al. (26) have demonstrated that the expression of the apical anion/HCO_3^- transport proteins downregulated in adenoma (DRA) and putative anion transporter (PAT1) is dependent on CFTR in the CFPAC-1 pancreatic duct line. It is therefore expected that HPAF cells, which express CFTR at very low

levels, would exhibit negligible amounts of anion/HCO_3^- transporters. Indeed, our preliminary RT-PCR experiments show, at best, very low levels of DRA, as well as the human pancreatic Na^+/HCO_3^- transporter, hpNBC (Fong P, Argent BA, Guggino WB, and Gray MA, unpublished observations). It will be interesting to ascertain whether overexpression of wild-type CFTR can upregulate anion transporters in HPAF cells, similar to what has been observed in CFPAC-1 cells (26).

Winpenny et al. (51) first identified CaCC in the HPAF cell line and in freshly isolated human pancreatic duct epithelial cells. Both ATP and ionomycin increase $[Ca^{2+}]_i$ in HPAF cells (1, 2), consistent with the increase in I_{sc} resulting from the activation of CaCC that is evoked by these stimulants (31, 51). Moreover, consistent with an apically localized CaCC, the addition of niflumic acid to the mucosal solution inhibited the ATP-stimulated I_{sc}. On the other hand, serosal niflumic acid addition did not indicate the presence of basolaterally localized CaCC. This observation is consistent with the reported inhibitory effect of the blocker on whole cell CaCC currents in HPAF cells (51). ATP-stimulated I_{sc} was increased in the presence of a serosal to mucosal Cl^- gradient. Taken together, these data suggest that CaCC mediates ATP-stimulated Cl^- secretion by HPAF cells and so must be expressed in the apical membrane.

What remains puzzling is our inability to detect mRNA encoding two molecularly identified members of the CLCA family of CaCCs (24). Given the limitations of RT-PCR, we cannot exclude the possibility that CLCA channels are expressed at a low level in HPAF cells. Alternatively, novel CaCCs, unrelated to the CLCA family, may be expressed or other known Cl^- channels may act as CaCCs in HPAF cells. RT-PCR analysis suggested the expression of both long and short splice variants of ClC-3 (38), ClC-5, and the positive control, ClC-2.

ClC-5 is an unlikely candidate for CaCC because it is unaffected by niflumic acid at concentrations up to 1 mM (47). It is also uncertain whether intracellular Ca^{2+} plays a role in the regulation of CLC-5. Friedrich et al. (23) noted that, when expressed in *Xenopus* oocytes, ClC-5 currents can be detected in EGTA-buffered intracellular solutions and therefore do not depend on intracellular Ca^{2+}. There is one report demonstrating regulation of CLC-3 via multifunctional Ca^{2+}/calmodulin kinase (28), and niflumic acid (500 μM) has been reported to block ~50% of the swelling activated Cl^- currents that resemble ClC-3 in renal inner medullary collecting duct cells (4).

ClC-3 and ClC-5 have an intracellular localization and function (50). This, together with the above points, speaks against the involvement of either channel in mediating CaCC. However, our Western blot experiments indicate the presence in HPAF cells of both ClC-3 and ClC-5 protein, as well as the ubiquitously distributed ClC-2. We note that CLC channels can form heteromeric assemblies (33) with unique functional properties. What remains to be tested systematically is whether such assemblies exist between ClC-2, ClC-3, and ClC-5 in native epithelial cells and whether these complexes can mediate a CaCC.

In contrast to the ATP-stimulated I_{sc}, the resting Cl^- conductance in HPAF cells is resistant to niflumic acid block. In principle, ClC-2, ClC-3, or ClC-5 represent possible candidates for mediating the resting conductance, as does the weakly expressed CFTR. The gating of ClC-2 is favored by membrane hyperpolarization, whereas depolarization favors the gating of ClC-3 and ClC-5. Replacement of mucosal Cl^-, which results in apical membrane depolarization, would favor ClC-3 and ClC-5 opening, whereas it would reduce that of ClC-2. However, the lack of a significant change in basal I_{sc} with mucosal Cl^- replacement suggests that no single channel/conductance serves as the exclusive apical conduits for Cl^-. Rather, their relative contributions would vary as a function of membrane potential, hence providing a constant net conductance.

We used specific blockers and activators of different classes of K^+ channels to identify the K^+ conductances in HPAF cells and to determine their role in maintaining the resting and ATP-stimulated I_{sc}. Clotrimazole, a blocker of Ca^{2+}-activated K^+ channels, inhibited both basal and ATP-stimulated I_{sc}. Saturating block could only be observed after addition of clotrimazole to both aspects of the monolayer, suggesting expression of Ca^{2+}-activated K^+ channels in both the serosal and mucosal membranes. To investigate whether maxi-K^+ channels were involved, we exposed HPAF monolayers to iberiotoxin and charybdotoxin. Neither toxin had any effect on I_{sc}, ruling out a contribution from this channel type. In contrast, chlorzoxazone, an activator of small and intermediate conductance Ca^{2+}-activated K^+ channels, stimulated I_{sc} strongly when added to the mucosal chamber but had little effect when delivered to the serosal side. These data suggest that small and intermediate conductance Ca^{2+}-activated K^+ channels are expressed not only in the serosal membrane of HPAF cells but also in the mucosal membrane. Moreover, these channels probably play a role in determining both the resting and the ATP-stimulated I_{sc}. The detection of KCNN4 in HPAF cells by RT-PCR is consistent with these findings.

Clofilium is a blocker of cAMP-activated K^+ channels (17, 18). We found that a clofilium-sensitive K^+ conductance was localized on the mucosal membrane of HPAF cells. Clofilium had no effect on ATP-stimulated I_{sc} but did significantly reduce basal I_{sc} levels. Cowley and Lindsdell (17) analyzed the block of I_{sc} by clofilium in Calu-3 cells. Their electrophysiological data and their RT-PCR studies confirmed the presence of KCNQ1 and KCNE3, previously identified components of an epithelial cAMP-activated K^+ channel (43). Because we were unable to detect strong expression of KCNQ1 in HPAF cells using RT-PCR, we tested the effects of chromanol 293B, a more specific inhibitor of epithelial cAMP-activated K^+ channels (3). Consistent with the RT-PCR data, 293B had no effect on I_{sc}. We thus conclude that a K^+ channel other than cAMP-regulated KCNQ1/KCNE complexes underlies the clofilium-sensitive current. Recently, Niemeyer et al. (35)

demonstrated a block of KCNK5 by clofilium, and our RT-PCR data indicate that KCNK5 (TASK2) is expressed in HPAF cells. KCNK5 (TASK2) is an acid-sensitive member of the 4TMD-2P family of K^+ channels and is markedly stimulated at alkaline extracellular pH (40).

Taken together, our data suggest the cellular model for HPAF cells shown in Fig. 8. As expected, CaCC and some CFTR are expressed on the mucosal membrane. Although we have not presented evidence for the nature of the basolateral Cl^- uptake mechanism in this study, our preliminary findings indicate a small bumetanide-sensitive component, very likely the Na-K-2Cl cotransporter (NKCC). It remains to be determined whether other Na^+-coupled uptake mechanisms, such as a combination of Na^+/H^+ and Cl^-/HCO_3^- exchangers, play a role. However, our novel finding is that K^+ channels are expressed not only in the serosal membrane but also the mucosal membrane. Clotrimazole-sensitive small and intermediate conductance Ca^{2+}-activated K^+ channels (possibly KCNN4) are expressed in both mucosal and serosal membranes. These channels support basal and ATP-stimulated I_{sc} as shown by the inhibitory effect of both mucosal and serosal clotrimazole. Moreover, activation of the mucosal Ca^{2+}-activated K^+ conductance with chlorzoxazone results in the generation of a substantial I_{sc}, equivalent in magnitude to that obtained with 50 μM ATP. Finally, a clofilium-sensitive K^+ conductance, possibly KCNK5 (hTASK2), is located in the mucosal membrane. Because mucosal clofilium blocks only resting and not ATP-stimulated I_{sc}, we suggest that the clofilium-sensitive channels contribute to the resting K^+ conductance of the HPAF cell.

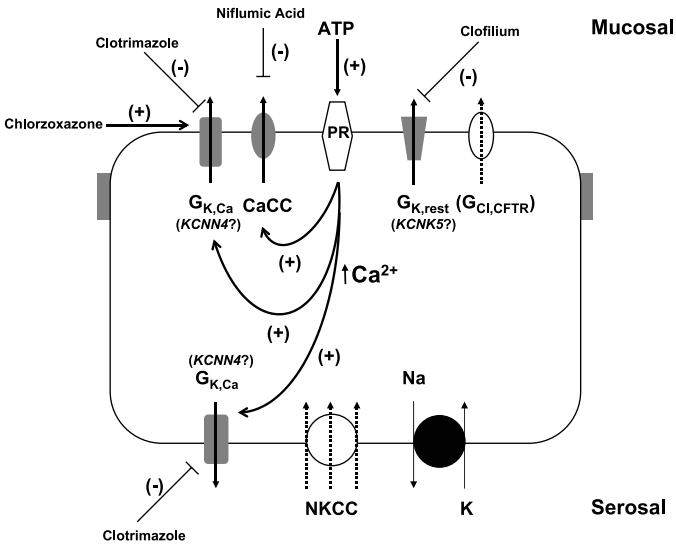

Fig. 8. Summary of Cl^- transport in HPAF cells. Resting I_{sc} is blocked maximally by bilateral clotrimazole. ATP, acting through a purinergic receptor (PR), stimulates I_{sc}. This increase is blocked by mucosal clotrimazole and niflumic acid. Resting I_{sc} also is inhibited by the action of mucosal clofilium on a basally active K^+ channel. Furthermore, mucosal chlorzoxazone elevates I_{sc}, an effect blocked by mucosal but not serosal clotrimazole. Taken together, the pharmacological and RT-PCR evidence suggest that the clotrimazole-sensitive, chlorzoxazone/ATP-activated K^+ conductance, $G_{K,Ca}$, is mediated by KCNN4 and the clofilium-sensitive, basal K^+ conductance, $G_{K,rest}$, by KCNK5. The present study *1*) localizes these 2 pharmacologically distinct K^+ conductances to the apical membrane and *2*) also provides evidence for a basolaterally situated, clotrimazole-sensitive K^+ conductance. The molecular identity of the Ca^{2+}-activated Cl^- conductance (CaCC) remains to be positively identified. Unlike native pancreatic ductal cells, contributions of CFTR to I_{sc} are negligible; this may be further limited by a reduced capacity to accumulate Cl^- intracellularly [designated by dotted arrows for both $G_{Cl,CFTR}$ and Na-K-2Cl cotransporter (NKCC)]. See text for further discussion.

As proposed by Cook and Young (16) and recently discussed by Wong (53), stimulation of an apical K^+ conductance in epithelial cells would depolarize V_t and ultimately enhance anion secretion by blunting the development of a rate-limiting lumen negative V_t. Thus the presence of KCNK5 (hTASK2) and a Ca^{2+}-activated K^+ conductance (KCNN4) on the mucosal membrane of pancreatic duct cells would be physiologically useful in terms of maintaining the electrical driving force for electrogenic HCO_3^- secretion. Interestingly, on stimulation by secretin, rat and rabbit pancreatic ductal secretions contain K^+ levels exceeding those in plasma (6, 32, 39, 45). Indeed, in the rat, juice K^+ concentrations equal to twice the plasma value have been observed after secretin stimulation (45). Our observation that an apical K^+ conductance exists in HPAF cells contrasts with results obtained by Novak and Greger (36) using the isolated, perfused rat pancreatic duct. In this preparation, the lack of V_t response to step changes in luminal K^+ led these investigators to argue against the notion of a luminal G_K. However, a mucosal K^+ conductance mediated by the pH-sensitive and clofilium-sensitive KCNK5 (hTASK2) (Fig. 8) may only become apparent as the concentration of HCO_3^- in the luminal fluid rises. Interestingly, the airway epithelium, a tissue in which the lack of functional CFTR results in severe disease, demonstrates appreciable apical pathways for K^+ movement (13, 19). This therefore raises the possibility that apical airway K^+ conductances also may be at least partially mediated by the pH-sensitive KCNK5.

In summary, we have shown that HPAF cells can be cultured to form a polarized monolayer that exhibits Cl^- secretion. As well as mucosal CaCC and CFTR Cl^- channels, the HPAF cells have K^+ channels in both their serosal and mucosal membranes. Our studies show the expression of CLC channels in HPAF cells, and the possibility that these may underlie CaCC remains to be systematically addressed. Based on RT-PCR studies and pharmacological data, we suggest that the Ca^{2+}-activated K^+ channel, KCNN4, is expressed at both membranes in HPAF cells, whereas RT-PCR, pharmacological, and immunoblot evidence support the notion that a pH-sensitive K^+ channel, KCNK5 (hTASK2), is expressed at the mucosal membrane only. Further electrophysiological studies, as well as direct antibody localization, will be required to confirm this hypothesis. Finally, we propose that the mucosal K^+ conductance, by limiting the hyperpolarization of V_t after the stimulation of secretion, may be important in maintaining electrogenic HCO_3^- secretion.

We thank Drs. Elizabeth Cowley, Catherine Fuller, Jie Cheng, Shao-Xiong Wang, Xuemei Zhang, and Sandra Guggino for generously sharing information, reagents, and discussions critical to the progress of this study.

DISCLOSURES

This work was supported by grants from the Cystic Fibrosis Foundation (W. B. Guggino), National Heart, Lung, and Blood Institute Grant HL-47122 (W. B. Guggino), Cystic Fibrosis Research, Inc. (P. Fong), and the Cystic Fibrosis Trust (B. E. Argent, M. A. Gray).

REFERENCES

1. **Adair J, Jackson K, Gray MA, and Argent BE.** The effects of protein kinase C on calcium mobilization in a human pancreatic duct cell line (HPAF) (Abstract). *J Physiol* 527: 25P, 2000.
2. **Adair J, Stephenson D, Kappler T, Gray MA, and Argent BE.** Anion secretion and intracellular calcium concentration in a human pancreatic duct cell line (HPAF) (Abstract). *J Physiol* 520: 29P, 1999.
3. **Bleich M and Warth R.** The very small conductance K^+ channel K_vLQT1 and epithelial function. *Pflügers Arch* 440: 202–206, 2000.
4. **Boese SH, Glanville M, Gray MA, and Simmons NL.** The swelling-activated anion conductance in the mouse renal inner medullary collecting duct cell line mIMCD-K2. *J Membr Biol* 177: 51–64, 2000.
5. **Bösl MR, Stein V, Hubner C, Zdebik AA, Jordt SE, Mukhopadhyay AK, Davidoff MS, Holstein AF, and Jentsch TJ.** Male germ cells and photoreceptors, both dependent on close cell-cell interactions, degenerate upon ClC-2 Cl^- channel disruption. *EMBO J* 20: 1289–1299, 2001.
6. **Caflisch CR, Solomon S, and Galey WR.** In situ micropuncture study of pancreatic duct pH. *Am J Physiol Gastrointest Liver Physiol* 238: G263–G268, 1980.
7. **Carew MA, Yang X, Schultz C, and Shears SB.** Myo-inositol 3,4,5,6-tetrakisphosphate inhibits an apical calcium-activated chloride conductance in polarized monolayers of a cystic fibrosis cell line. *J Biol Chem* 275: 26906–26913, 2000.
8. **Chambers JA and Harris A.** Expression of the cystic fibrosis gene and the major pancreatic mucin gene, MUC1, in human ductal epithelial cells. *J Cell Sci* 105: 417–422, 1993.
9. **Cheng HS, Wong WS, Chan KT, Wang XF, Wang ZD, and Chan HC.** Modulation of Ca^{2+}-dependent anion secretion by protein kinase C in normal and cystic fibrosis pancreatic duct cells. *Biochim Biophys Acta* 1418: 31–38, 1999.
10. **Chillon M, Casals T, Mercier B, Bassas L, Lissens W, Silber S, Romey MC, Ruiz-Romero J, Verlingue C, Claustres M, Nunes V, Ferec C, and Estivill X.** Mutations in the cystic fibrosis gene in patients with congenital absence of the vas deferens. *N Engl J Med* 332: 1475–1480, 1995.
11. **Choo-Kang LR and Zeitlin PL.** Type I, II, III, IV, and V cystic fibrosis transmembrane conductance regulator defects and opportunities for therapy. *Curr Opin Pulm Med* 6: 521–529, 2000.
12. **Choudari CP, Lehman GA, and Sherman S.** Pancreatitis and cystic fibrosis gene mutations. *Gastroenterol Clin North Am* 28: 543–549, 1999.
13. **Clarke LL, Chinet T, and Boucher RC.** Extracellular ATP stimulates K^+ secretion across cultured human airway epithelium. *Am J Physiol Lung Cell Mol Physiol* 272: L1084–L1091, 1997.
14. **Cohn JA, Friedman KJ, Noone PG, Knowles MR, Silverman LM, and Jowell PS.** Relation between mutations of the cystic fibrosis gene and idiopathic pancreatitis. *N Engl J Med* 339: 653–658, 1998.
15. **Conway SP, Peckham DG, Chu CE, Ellis LA, Ahmed M, and Taylor GR.** Cystic fibrosis presenting as acute pancreatitis and obstructive azoospermia in a young adult male with a novel mutation in the CFTR gene. *Pediatr Pulmonol* 34: 491–495, 2002.
16. **Cook DI and Young JA.** Effect of K^+ channels in the apical plasma membrane on epithelial secretion based on secondary active Cl^- transport. *J Membr Biol* 110: 139–146, 1989.
17. **Cowley EA and Linsdell P.** Characterization of basolateral K^+ channels underlying anion secretion in the human airway cell line Calu-3. *J Physiol* 538: 747–757, 2002.
18. **Devor DC, Bridges RJ, and Pilewski JM.** Pharmacological modulation of ion transport across wild-type and ΔF508 CFTR-expressing human bronchial epithelia. *Am J Physiol Cell Physiol* 279: C461–C479, 2000.
19. **Devor DC, Singh AK, Lambert LC, DeLuca A, Frizzell RA, and Bridges RJ.** Bicarbonate and chloride secretion in Calu-3 human airway epithelial cells. *J Gen Physiol* 113: 743–760, 1999.
20. **Dowland LK, Luyckx VA, Enck AH, Leclercq B, and Yu AS.** Molecular cloning and characterization of an intracellular chloride channel in the proximal tubule cell line, LLC-PK1. *J Biol Chem* 275: 37765–37773, 2000.
21. **Dray X, Zinzindohoue F, Cuillerier E, Cugnenc PH, Barbier JP, and Marteau P.** Acute pancreatitis revealing cystic fibrosis in an adult. *Gastroenterol Clin Biol* 23: 974–977, 1999.
22. **Durie PR and Forstner GG.** Pathophysiology of the exocrine pancreas in cystic fibrosis. *J R Soc Med* 82: 2–10, 1989.
23. **Friedrich T, Breiderhoff T, and Jentsch TJ.** Mutational analysis demonstrates that ClC-4 and ClC-5 directly mediate plasma membrane currents. *J Biol Chem* 274: 896–902, 1999.
24. **Fuller CM and Benos DJ.** Electrophysiological characteristics of the Ca^{2+}-activated Cl^- channel family of anion transport proteins. *Clin Exp Pharmacol Physiol* 27: 906–910, 2000.
25. **Gray MA, Winpenny JP, Porteous DJ, Dorin JR, and Argent BE.** CFTR and calcium-activated chloride currents in pancreatic duct cells of a transgenic CF mouse. *Am J Physiol Cell Physiol* 266: C213–C221, 1994.
26. **Greeley T, Shumaker H, Wang Z, Schweinfest CW, and Soleimani M.** Downregulated in adenoma and putative anion transporter are regulated by CFTR in cultured pancreatic duct cells. *Am J Physiol Gastrointest Liver Physiol* 281: G1301–G1308, 2001.
27. **Holliday ND and Cox HM.** Modulation of chloride, potassium and bicarbonate transport by muscarinic receptors in a human adenocarcinoma cell line. *Br J Pharmacol* 126: 269–279, 1999.
28. **Huang P, Liu J, Di A, Robinson NC, Musch MW, Kaetzel MA, and Nelson DJ.** Regulation of human CLC-3 channels by multifunctional Ca^{2+}/calmodulin-dependent protein kinase. *J Biol Chem* 276: 20093–20100, 2001.
29. **Joiner WJ, Wang LY, Tang MD, and Kaczmarek LK.** hSK4, a member of a novel subfamily of calcium-activated potassium channels. *Proc Natl Acad Sci USA* 94: 11013–11018, 1997.
30. **Kim YW, Kern HF, Mullins TD, Koriwchak MJ, and Metzgar RS.** Characterization of clones of a human pancreatic adenocarcinoma cell line representing different stages of differentiation. *Pancreas* 4: 353–362, 1989.
31. **Lindgard JM, Stephenson D, Kappler T, Jackson KA, Windass AS, Gray MA, and Argent BE.** Ca^{+2}-mediated anion secretion from human pancreatic duct cells and its inhibition by protein kinase C (Abstract). *Ped Pulmonol Suppl* S20: 205, 2000.
32. **Lingard JM and Young JA.** β-Adrenergic control of exocrine secretion by perfused rat pancreas in vitro. *Am J Physiol Gastrointest Liver Physiol* 245: G690–G696, 1983.
33. **Lorenz C, Pusch M, and Jentsch TJ.** Heteromultimeric CLC chloride channels with novel properties. *Proc Natl Acad Sci USA* 93: 13362–13366, 1996.
34. **Merlin D, Jiang L, Strohmeier GR, Nusrat A, Alper SL, Lencer WI, and Madara JL.** Distinct Ca^{2+}- and cAMP-dependent anion conductances in the apical membrane of polarized T84 cells. *Am J Physiol Cell Physiol* 275: C484–C495, 1998.
35. **Niemeyer MI, Cid LP, Barros LF, and Sepulveda FV.** Modulation of the two-pore domain acid-sensitive K^+ channel TASK-2 (KCNK5) by changes in cell volume. *J Biol Chem* 276: 43166–43174, 2001.
36. **Novak I and Greger R.** Effect of bicarbonate on potassium conductance of isolated perfused rat pancreatic ducts. *Pflügers Arch* 419: 76–83, 1991.
37. **Novak I and Hansen MR.** Where have all the Na^+ channels gone? In search of functional ENaC in exocrine pancreas. *Biochim Biophys Acta* 1566: 162–168, 2002.

38. **Ogura T, Furukawa T, Toyozaki T, Yamada K, Zheng YJ, Katayama Y, Nakaya H, and Inagaki N.** ClC-3B, a novel ClC-3 splicing variant that interacts with EBP50 and facilitates expression of CFTR-regulated ORCC. *FASEB J* 16: 863–865, 2002.
39. **Perlmutter J and Martinez JR.** The chronically reserpinized rat as a possible model for cystic fibrosis. VII. Alterations in the secretory response to cholecystokinin and to secretin from the pancreas in vivo. *Pediatr Res* 12: 188–194, 1978.
40. **Reyes R, Duprat F, Lesage F, Fink M, Salinas M, Farman N, and Lazdunski M.** Cloning and expression of a novel pH-sensitive two pore domain K^+ channel from human kidney. *J Biol Chem* 273: 30863–30869, 1998.
41. **Riordan JR, Rommens JM, Kerem B, Alon N, Rozmahel R, Grzelczak Z, Zielenski J, Lok S, Plavsic N, Chou JL, Drumm ML, Iannuzzi MC, Collins FS, and Tsui LC.** Identification of the cystic fibrosis gene: cloning and characterization of complementary DNA. *Science* 245: 1066–1073, 1989.
42. **Schoumacher RA, Ram J, Iannuzzi MC, Bradbury NA, Wallace RW, Hon CT, Kelly DR, Schmid SM, Gelder FB, Rado TA, and Frizzell RA.** A cystic fibrosis pancreatic adenocarcinoma cell line. *Proc Natl Acad Sci USA* 87: 4012–4016, 1990.
43. **Schroeder BC, Hechenberger M, Weinreich F, Kubisch C, and Jentsch TJ.** KCNQ5, a novel potassium channel broadly expressed in brain, mediates M-type currents. *J Biol Chem* 275: 24089–24095, 2000.
44. **Schwake M, Friedrich T, and Jentsch TJ.** An internalization signal in ClC-5, an endosomal Cl-channel mutated in Dent's disease. *J Biol Chem* 276: 12049–12054, 2001.
45. **Sewell WA and Young JA.** Secretion of electrolytes by the pancreas of the anaesthetized rat. *J Physiol* 252: 379–396, 1975.
46. **Singh AK, Devor DC, Gerlach AC, Gondor M, Pilewski JM, and Bridges RJ.** Stimulation of Cl^- secretion by chlorzoxazone. *J Pharmacol Exp Ther* 292: 778–787, 2000.
47. **Steinmeyer K, Schwappach B, Bens M, Vandewalle A, and Jentsch TJ.** Cloning and functional expression of rat CLC-5, a chloride channel related to kidney disease. *J Biol Chem* 270: 31172–31177, 1995.
48. **Stobrawa SM, Breiderhoff T, Takamori S, Engel D, Schweizer M, Zdebik AA, Bösl MR, Ruether K, Jahn H, Draguhn A, Jahn R, and Jentsch TJ.** Disruption of ClC-3, a chloride channel expressed on synaptic vesicles, leads to a loss of the hippocampus. *Neuron* 29: 185–196, 2001.
49. **Thomas EJ, Gabriel SE, Makhlina M, Hardy SP, and Lethem MI.** Expression of nucleotide-regulated Cl^- currents in CF and normal mouse tracheal epithelial cell lines. *Am J Physiol Cell Physiol* 279: C1578–C1586, 2000.
50. **Wills NK and Fong P.** ClC chloride channels in epithelia: recent progress and remaining puzzles. *News Physiol Sci* 16: 161–166, 2001.
51. **Winpenny JP, Harris A, Hollingsworth MA, Argent BE, and Gray MA.** Calcium-activated chloride conductance in a pancreatic adenocarcinoma cell line of ductal origin (HPAF) and in freshly isolated human pancreatic duct cells. *Pflügers Arch* 435: 796–803, 1998
52. **Winpenny JP, Verdon B, McAlroy HL, Colledge WH, Ratcliff R, Evans MJ, Gray MA, and Argent BE.** Calcium-activated chloride conductance is not increased in pancreatic duct cells of CF mice. *Pflügers Arch* 430: 26–33, 1995.
53. **Wong PYD.** Do seminiferous tubules secrete a fluid rich in $KHCO_3$? *J Physiol* 542: 335, 2002.
54. **Zsembery Á, Strazzabosco M and Graf J.** Ca^{2+}-activated Cl^- channels can substitute for CFTR in stimulation of pancreatic duct bicarbonate secretion. *FASEB J* 14: 2345–2356, 2000.